Jikeikai Med J 2007 ; 54 : 177-88

Ultrastructural Features of Human Intraepidermal Nerve Fibers with a Focus on the Intercellular Space

Toshiaki HIRAI[1], Masahiro KANBE[2], Hidemi NAKAGAWA[2],
Toshio SAKAI[3], and Kiyoharu INOUE[1]

[1]*Division of Neurology, Department of Internal Medicine, The Jikei University School of Medicine*
[2]*Department of Dermatology, The Jikei University School of Medicine*
[3]*SAKAI Electron Microscopy Application Laboratory*

ABSTRACT

To clarify the ultrastructural features of human intraepidermal nerve fibers (IENFs), we performed examinations by electron microscopy and confocal laser scanning microscopy. Skin specimens were obtained from a healthy subject and fixed for each study. Confocal laser scanning microscopic examination showed that IENFs were immunohistochemically stained for protein gene product 9.5 and ran through the epidermal intercellular space. Electron microscopic examination demonstrated little shrinkage of keratinocytes, interdigitations of microvilli, and processes of keratinocytes, axons, melanocytes, and Langerhans cells in the spaces between keratinocytes. Axon had low electron density and few identifiable organelles without a basement membrane or Schwann cells, and were directly apposed to the plasma membrane of keratinocytes. Unlike other processes, axons did not have large intercellular spaces. In conclusion, this study has demonstrated the ultrastructural features of human IENFs and of other cellular processes with a focus on the intercellular space. Differences in the intercellular space can be used to distinguish axons from other cellular processes. (Jikeikai Med J 2007 ; 54 : 177-88)

Key words : ultrastructure, intraepidermal nerve fiber, human epidermis, cell process, intercellular space

INTRODUCTION

For more than a century, there has been a controversy regarding human intraepidermal nerve fibers (IENFs)[1-6]. Many techniques, including electron microscopy (EM) has been used to examine IENFs ; however, technical problems, which have not been described in detail, have prevented the identifications of IENFs in skin specimens from being reproduced reliably. Therefore, until the late 1980s nerve endings were generally believed not to penetrate the dermal-epidermal junction.

After the early 1990s, confocal laser scanning microscopy (CLSM) with the immunohistochemical marker protein gene product (PGP) 9.5 showed that IENFs are abundant in human epidermis[7], and this technique has become a useful method for evaluating skin innervation and painful neuropathy[8-12].

On the other hand, EM study of human IENFs has made little progress. Kennedy et al[7] demonstrated IENFs by means of EM but did not perform ultrastructural immunohistochemical studies. Therefore, ultrastructural features of IENFs could not be observed in detail, and IENFs in the epidermis could not

Received for publication, October 30, 2007
平井　利明，神部　正博，中川　秀已，酒井　俊男，井上　聖啓
Mailing address : Toshiaki HIRAI, Division of Neurology, Department of Internal Medicine, The Jikei University School of Medicine, 3-25-8, Nishi-Shimbashi, Minato-ku, Tokyo 105-8461, Japan.
E-mail : CYL07761@nifty.ne.jp

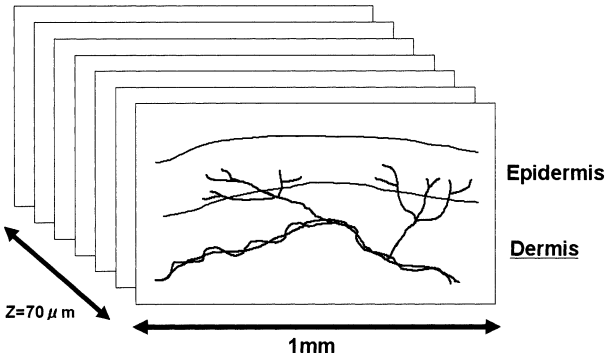

Fig. 1. A schematic diagram of PGP-9.5-positive fibers. The fibers penetrate the dermal-epidermal junction and are present as IENFs in the epidermis. The linear density of IENFs is calculated with the whole thickness of specimens sectioned toward the Z-axis. This figure was reprinted[12] with permission from Japanese Peripheral Nerve Society.

easily be detected because keratinocytes shrank with 0.1 M phosphate buffer (PB). Hilliges et al[13] demonstrated human IENFs through ultrastructural immunohistochemical studies but also found large intercellular spaces between keratinocytess, resulting in a failure to examine IENFs or the plasma membranes of the surrounding cells in detail.

In the present study we performed: 1) a CLSM examination of IENFs stained with PGP 9.5 at 2 lesions (distal leg and the abdomen) to identify axons for EM study and 2) an EM study, with a low concentration of PB, to observe the ultrastructural features of human epidermis, with a focus on the intercellular space.

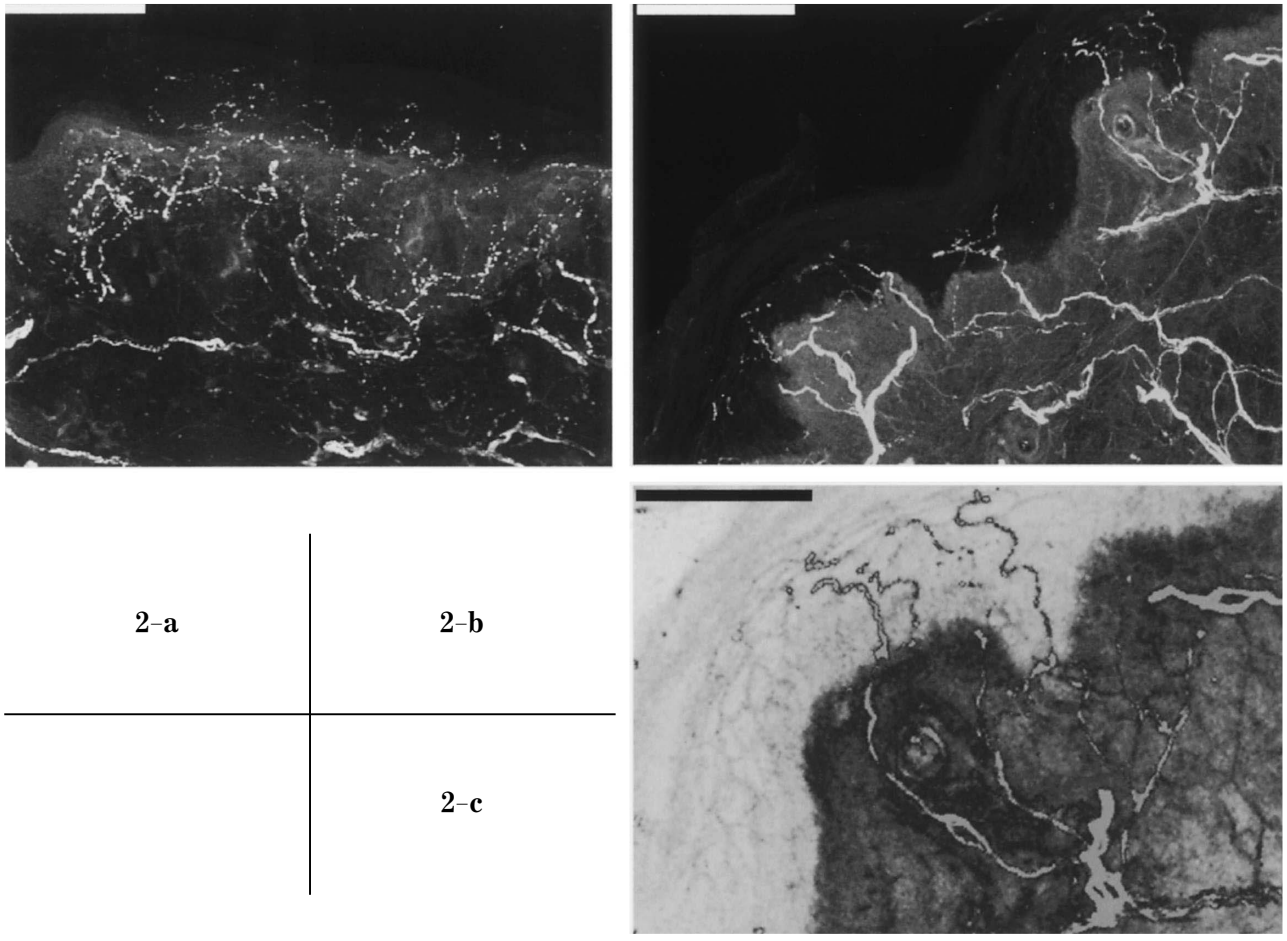

Fig. 2. Fibers stained for PGP 9.5 were observed in skin from the abdomen (2-a, bar=100 μm) and skin from the distal leg (2-b, bar=100 μm). The fibers penetrated the dermal-epidermal junction and were more abundant in abdominal skin than in leg skin. They ran through the intercellular space (2-c, bar=50 μm). This figure was reprinted[12] with permission from Japanese Peripheral Nerve Society.

Materials and Method

Four-millimeter-diameter punch biopsy specimens were obtained from the skin of the distal leg (10 cm above the lateral malleolus) and the abdomen (5 cm lateral to the navel) of a healthy male volunteer (aged 29 years) after injection of 1% xylocaine 5 mm from each biopsy site. The specimens were fixed for EM and immunohistochemical study, respectively.

Specimens for immunohistochemical study were immersed in a fixative containing 4% paraformaldehyde for 3 to 7 days, diluted with 0.4 M PB and 16% paraformaldehyde (Electron Microscopy Sciences, Hatfield, PA, USA) for 2 hours at room temperature, then cryoprotected in 0.1 M phosphate-buffered saline (PBS, pH 7.4) containing 20% sucrose overnight at 4BC and embedded. Sections were cut perpendicular to the skin surface with a cryostat (HM505E, Microm International GmbH, Walldorf, Germany). Thick sections (70 μm) were processed in PBS containing 0.3% Triton X-100 (PBST, pH 7.4) while floating free. Specimens were incubated in 10% H_2O_2 in PBST overnight at 4°C to obtain clear images. After preincubation in 10% normal goat serum in 0.1% PBST for 2 hours, the sections were incubated at 4°C with a polyclonal rabbit antibody against PGP 9.5 (1 : 5,000, UltraClone Ltd., Lucigen Corp., Middleton, WI, USA). The sections were washed in 0.1% PBST and incubated for 2 hours with a goat anti-rabbit IgG conjugated to fluorescein isothiocyanate (1 : 200, Jackson ImmunoResearch Laboratories, Inc., West Grove, PA, USA). Following additional washes, sections were coverslipped with mixed solutions of PBS and glyceol (1 : 1). Confocal images were obtained with a CLSM (LSM510, Carl Zeiss, Oberkochen, Germany) and 10× and 20× objective lenses (0.5 and 0.75 NA ; Plan-Apochromat, Carl Zeiss).

Specimens for EM were immersed in a fixative containing 1% glutaraldehyde in 0.08 M phosphate buffer (PB) (pH 7.4) for 2 hours at room temperature. They were rinsed in buffer for 60 minutes and postfixed with 1% osmium tetroxide in 0.1 M PB for 60 minutes. After these procedures, the tissue block was dehydrated through a series of ethanols for 10 minutes as follows ; 50%, 70%, 80%, 90%, 95%, 100%, 100%, 100%. The tissue block was then transferred to propylene oxide and embedded in epoxy resin, mixing A and B in the ratio of 4 : 6 measured by weight, based on the method of Luft[14]. Ultrathin sections were cut parallel to the skin surface on an ultramicrotome (ULTRACUT S, Leica Microsystems GmbH, Wetzlar, Germany) and double-stained with 1% uranyl acetate and 0.1% lead citrate. The ultrathin sections were observed and photographed with a transmission EM (H-7100, Hitachi Medical Corp., Tokyo).

CLSM study

The linear density of IENFs (number/mm) is expressed as the number of fibers per linear millimeter of epidermis penetrating dermal-epidermal junctions, with the whole thickness sectioned toward the Z-axis at 1.0-μm intervals (image size, 1,024× 1,024 pixels, Fig. 1), and determined in consecutive sections at 9 fields taken from abdominal or distal leg skin. Statisitical signigicance of these IENFD was assessed by Mann-Whitney U-test test. A level of $p < 0.01$ was accepted as statistically significant.

EM study

Biopsies for EM were performed where PGP-9.5-positive fibers were abundant at 1 of 2 lesions on CLSM. Observations were performed with 9.4× enlargements of negatives of photographs taken at 1,000× magnification and with higher-magnification photographs or digital images of positive photographs. In the epidermis, the observation focused on 1) the intercellular space of keratinocytes, 2) surrounding structures, 3) and the relationships of interdigitations between membranes of cell processes and membranes of keratinocytes.

Results

CLSM study

Fibers immunohistochemically stained for PGP 9.5 were observed in skin from the abdomen (Fig. 2-a) and the distal leg (Fig. 2-b). The fibers penetrated the dermal-epidermal junction and were more abundant in abdominal skin than in the epidermis of the

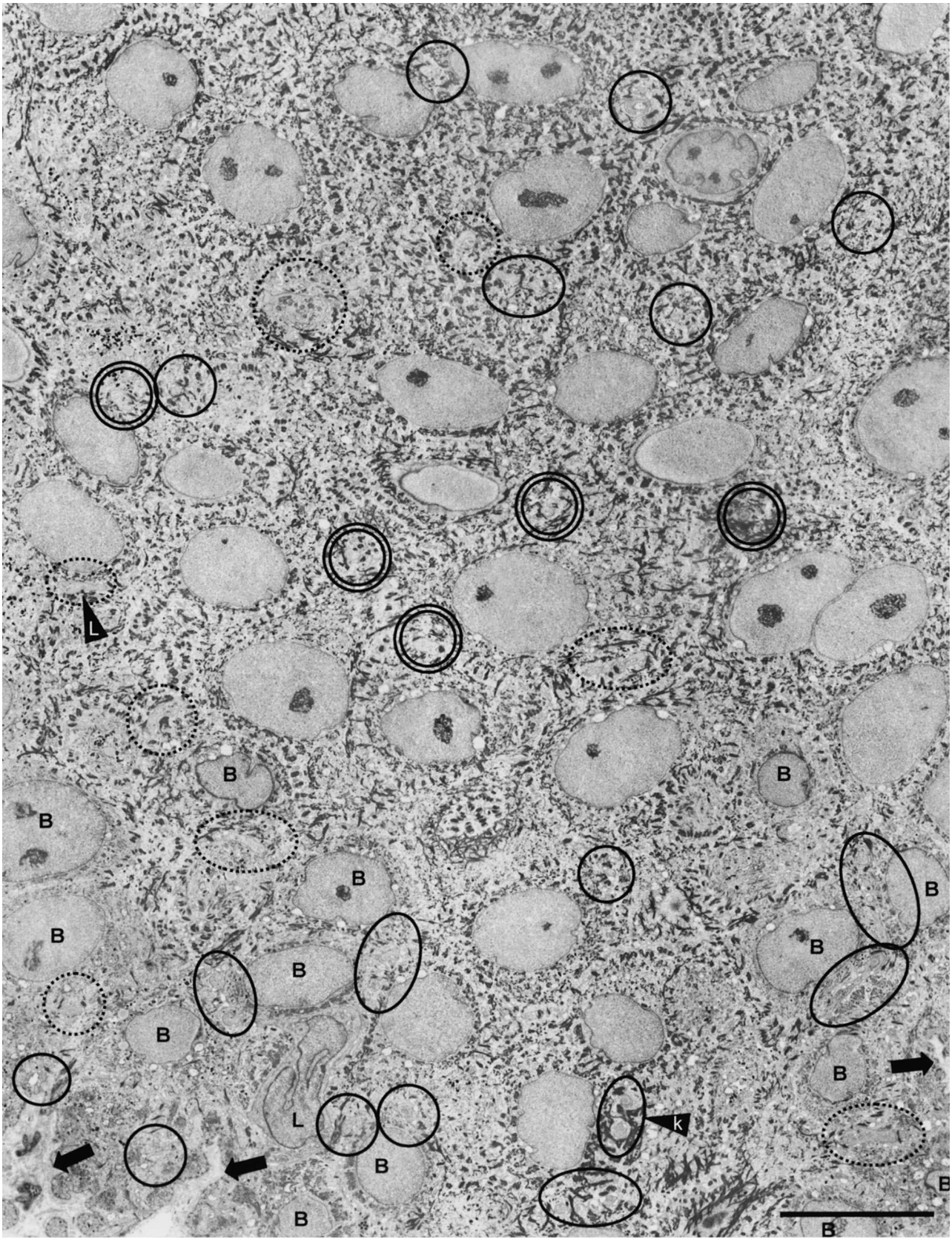
L
B
B
B
B
B
B
B
B
B
B
B
B
L
B
B
k
B
B
B

distal leg. The fibers ran through the intercellular space (Fig. 2-c). The linear density of IENFs was 32.0±2.2 (mean±SD) in abdominal skin and 17.4±2.2 in distal-leg skin (Mann-Whitney, $p<0.01$).

EM study

The EM studies were performed with abdominal skin from areas where abundant IENFs had been identified with CLSM. We obtained ultrastructural images of human epidermis, as shown in Fig. 3, 4, 5, 6, 7, and 8.

Fig. 3 shows a horizontal image of human abdominal skin (1,000× magnification). At the bottom of Fig. 3, dermal papillae are indicated by arrows. From the center to the top, a layer of keratinocytes located at the same horizontal level as the top of the dermal papillae is seen. Near these arrows are keratinocytes of the stratum basale, the nuclei of which are indicated with "B" and were found with part of the basement membrane. In these basal keratinocytes, some tonofilaments and desmosomes were found. The cytoplasm of these cells had a higher electronic density and was darker than the cytoplasm of squamous cells. The stratum spinosum extended around the stratum basale were occupied by squamous cells and showed abundant desmosomes and tonofilaments. The stratum granulosum, whose cells were filled with keratohyaline granules, was not included. The stratum corneum could not be included because a sufficiently large area could not be observed at 1,000× magnification because of poor permeation by the epoxy resin. Other arrows and circles will be described later.

Keratinocytes of the stratum spinosum showed little shrinkage (Fig. 4, 2,000× magnification). Desmosomes as junctional complexes were abundant between adjacent keratinocytes, and microvilli were present as interdigitations among them. An arrow indicates a group B process (described later). Fig. 3 and 4 show 4 types of cell processes in the interdigitating folds of the narrow intercellular space separating the apposed lateral surfaces of keratinocytes.

Group A processes (Fig. 5) had a high electron density and many organelles, such as ribosomes, with a keratinocytic matrix. Fig. 5 also includes the nucleus of a keratinocyte (stratum spinosum) as described below, and shows desmosomes with 3 plasma membranes of keratinocytes. When the "cleft" was defined as an artifitial structure in the intercellular space on fixation (see discussion), Group A processes had large clefts in the spaces between adjacent keratinocytes.

Group B processes had an extremely low electron density and few identifiable organelles, such as microtubules, some filaments, and mitochondria (Fig. 6-a, 6-b, 6-c). They are also indicated by arrows in Fig. 4. Fig. 6-a shows group B processes surrounded by the plasma membrane of a keratinocyte (stratum spinosum). There are desmosomes with group B processes in Fig. 6-b. In Fig. 6-c, interdigitations of microvilli are shown, and group B processes are adjacent to the plasma membranes of 2 keratinocytes (stratum spinosum). Clefts were few or absent in the spaces between adjacent keratinocytes.

Group C processes (Fig. 7) had a slightly low electron density with Birbeck granules (arrowhead), did not have pinocytotic vesicles, and were adjacent to 4 membranes of keratinocytes with a nucleus of a keratinocyte, as described below. Group C processes had some clefts in the spaces between adjacent keratinocytes.

Group D processes (Fig. 8) had many organelles with pinocytotic vesicles (arrowhead) and melanosomes. The processes were adjacent to the membranes of 3 keratinocytes with 3 nuclei. Group D processes had some clefts in the spaces between adjacent keratinocytes.

Only the membrane of group B processes seemed

Fig. 3. Horizontal image of human abdominal skin (1,000× magnification). At the bottom dermal papillae are indicated with arrows. Around these arrows, keratinocyte nuclei at the stratum basale are indicated with "B". Group A processes are indicated with circles, group B processes with double circles, and group C processes with dotted circles. A group A process shown in Fig. 5 is indicated by arrowhead "K", and a group C process shown in Fig. 7 is indicated by arrowhead "L". The nucleus of a Langerhans cell is indicated by "L" (bar=10 μm).

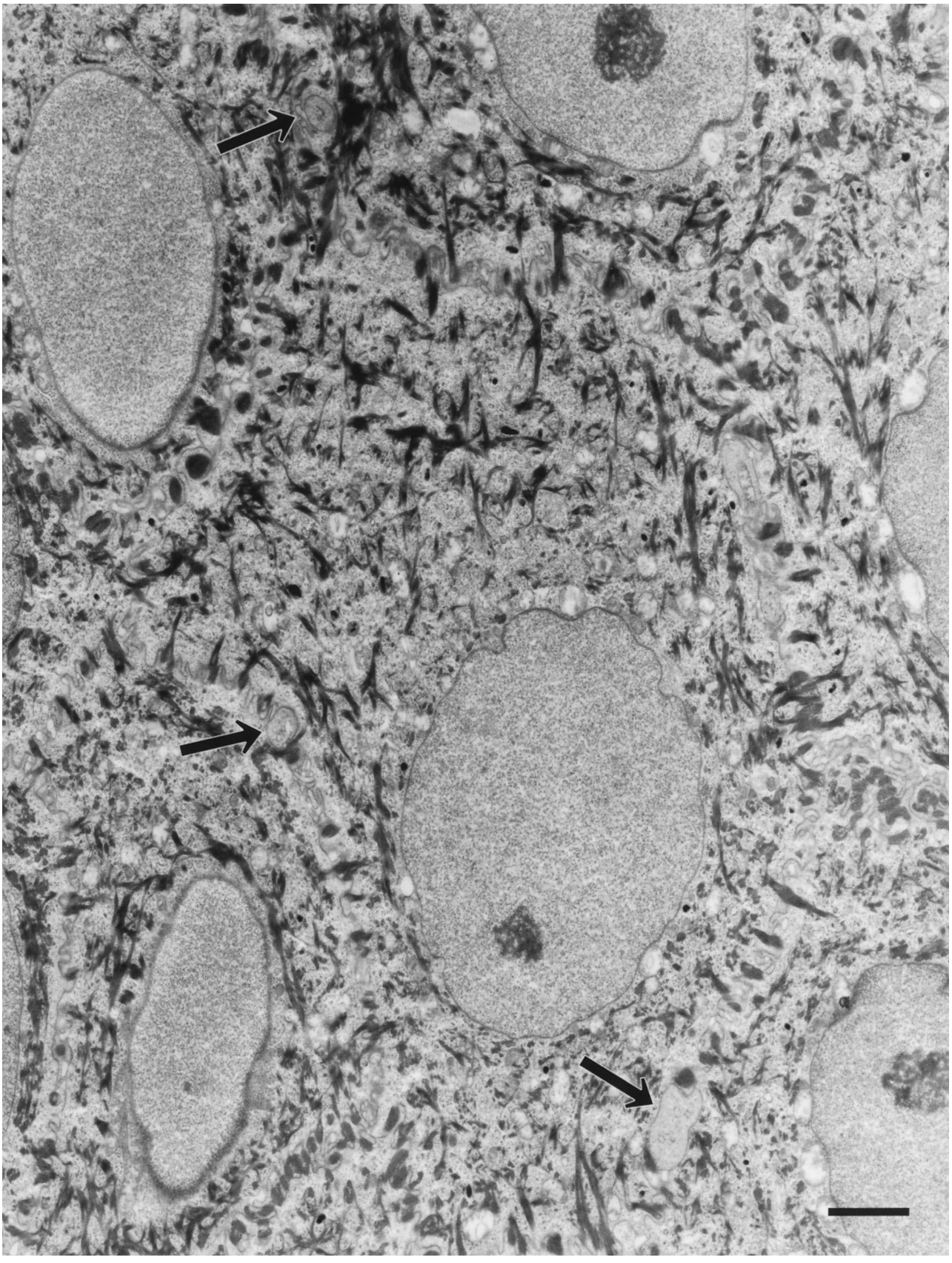

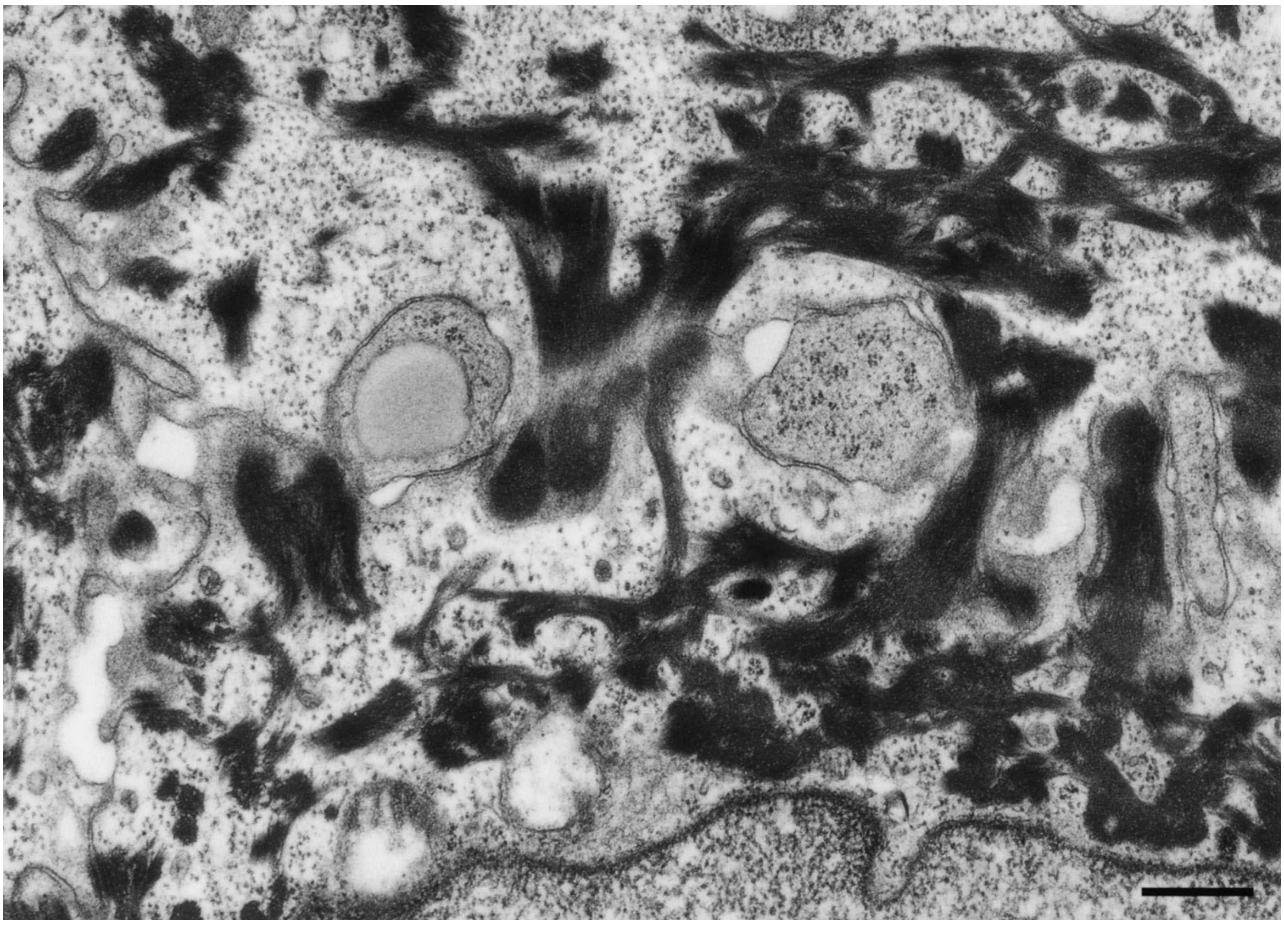

Fig. 5. Group A processes had a high electron density and many organelles within a keratinocytic matrix (bar= 500 nm). Large clefts in the spaces between adjacent keratinocytes are shown.

to be smooth, whereas membranes of other groups appeared rough. On the other hand, the processes seemed to be similar between group B and group C without Birbeck granules and between group A and group D without melanosomes. None of these cell processes was surrounded by Schwann cells or a basement membrane, and Merkel cell granules were not identified.

On the basis of the above observations, additional cell processes were identified in Fig. 3; group A processes are indicated with circles, group B processes are indicated with double circles, and group C processes are indicated with dotted circles. A group A process shown in Fig. 5 is indicated by arrowhead "K", and a group C process shown in Fig. 7 is indicated by arrowhead "L." Group D processes were not found in Fig. 3. Intercellular bridges, which are thought to be artifacts caused by shrinkage of keratinocytes on fixation, were not detected anywhere.

Discussion

Our CLSM study demonstrated that the linear density of IENFs was higher in skin from the abdomen than in skin from the distal leg. Wendelschafer-Crabb et al.[15] have reported that the linear density of IENFs is higher at proximal sites than at distal sites in humans, consistent with our results. Our concerns

Fig. 4. Ultrastructural image of human abdominal epidermis sectioned parallel to the skin surface showed little shrinkage of keratinocytes, microvilli as interdigitatations, and desmosomes as junctional complexes (bar= 2 μm). Group B processes are also indicated with arrows.

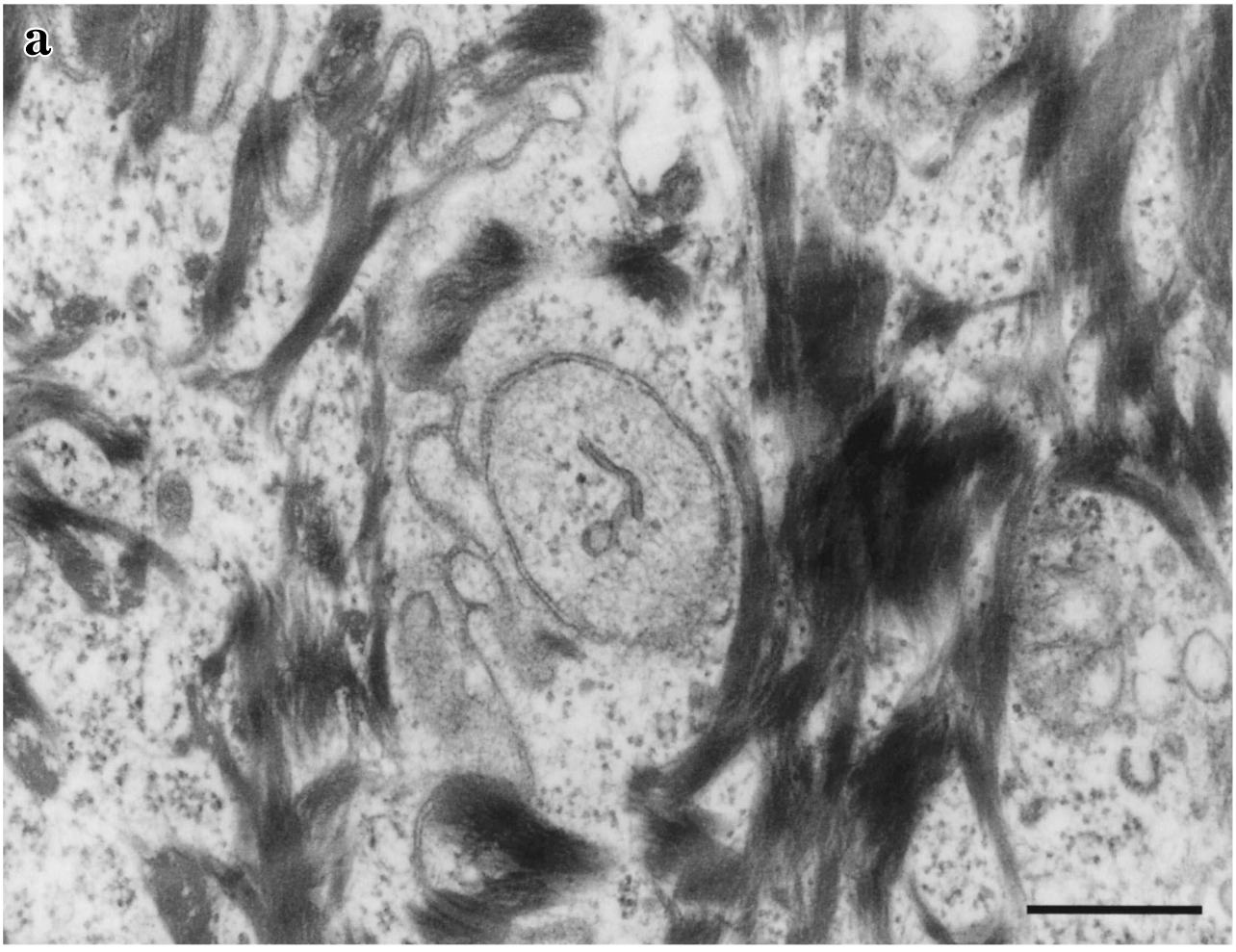

for EM study were mainly directed toward intercellular spaces, as shown in Fig. 2-c.

Group A processes had high electron density and many organelles, such as mitochondria, rough endoplasmic reticula, and vesicles, within a keratinocytic matrix. Therefore, we considered group A processes to be processes of keratinocytes. Group B processes, with an extremely low electron density and few identifiable organelles but without Birbeck granules, could be processes of axons. Group C processes clearly represented processes of Langerhans cells, with a cytoplasm containing Birbeck granules. Group D processes were identified as processes with pinocytotic vesicles. This classification of processes is similar to that in a previous study[13]. Group B were possibly axons; however, it was difficult to distinguish group B processes from other processes without ultrastructural immunohistochemical studies.

Differentiation between group B and group C processes without Birbeck granules and between group A and group D processes without melanosomes was difficult. When Birbeck granules were not detected in the cytoplasm on ultrathin sections, as in Fig. 3, the process was identified as that of a Langerhans cell after we confirmed that the cell was the same as that with Birbeck granules in another serial section and was at the stratum basale near the dermis. The nucleus of a Langerhans cell is indicated with an "L" in Fig. 3. Group D processes were not found in Fig. 3; however, we detected group D processes deep in the direction of epidermal prolongation through serial ultrathin sections.

Significance of "clefts"

Intercellular bridge is an artifactual structure that appears to be desmosome in the intercellular

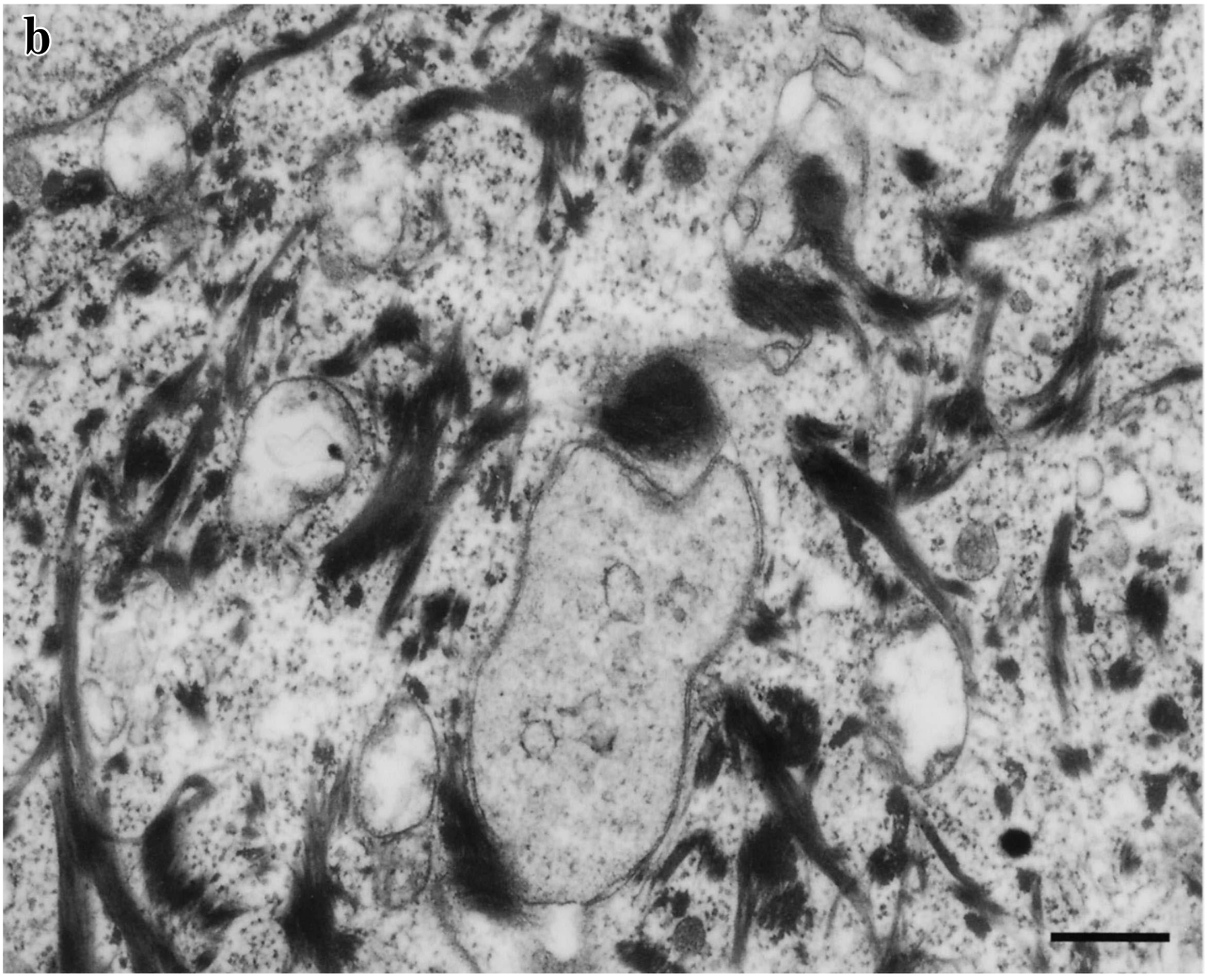

space when keratinocytes shrink strongly. Hilliges et al.[13] showed the ultrastructure of axon in the epidermis, however, the axon existed with intercellular bridge in the large intercellular space, resulting in a failure to observe intercellular space.

It is generally believed that intercellular space is a space from 10 to 20 nanometers. In our conditions of 0.08 M PB on the fixation, however, intercellular bridge were not found anywhere, and it was possible to prevent keratinocyte from shrinkage strongly and demonstrate usual intercellular space such as shown in Fig. 6a–c.

Even if the use of 0.08 M PB, group A processes, considered as processes of keratinocytes, had larger intercellular space than 10 to 20 nanometers. When this intercellular space was defined as "cleft", we found that axons had few or no clefts in the spaces between adjacent keratinocytes whereas other processes had some clefts.

We believe that cleft is a fixative artifact and significant findings, allowing axons and other processes to be distinguished. Furthermore, group B processes were not rough but were circular or elliptical structure. Therefore, group B processes should be considered axons even without ultrastructural immunohistochemical studies.

Determining the function of IENFs is extremely difficult. In some conditions, such as diabetic neuropathy and painful neuropathy, IENFs are less prevalent in the skin of the distal leg[8–10,12], indicating IENFs with EM was thought to be easier to be found when the biopsy site was the abdomen rather than the distal

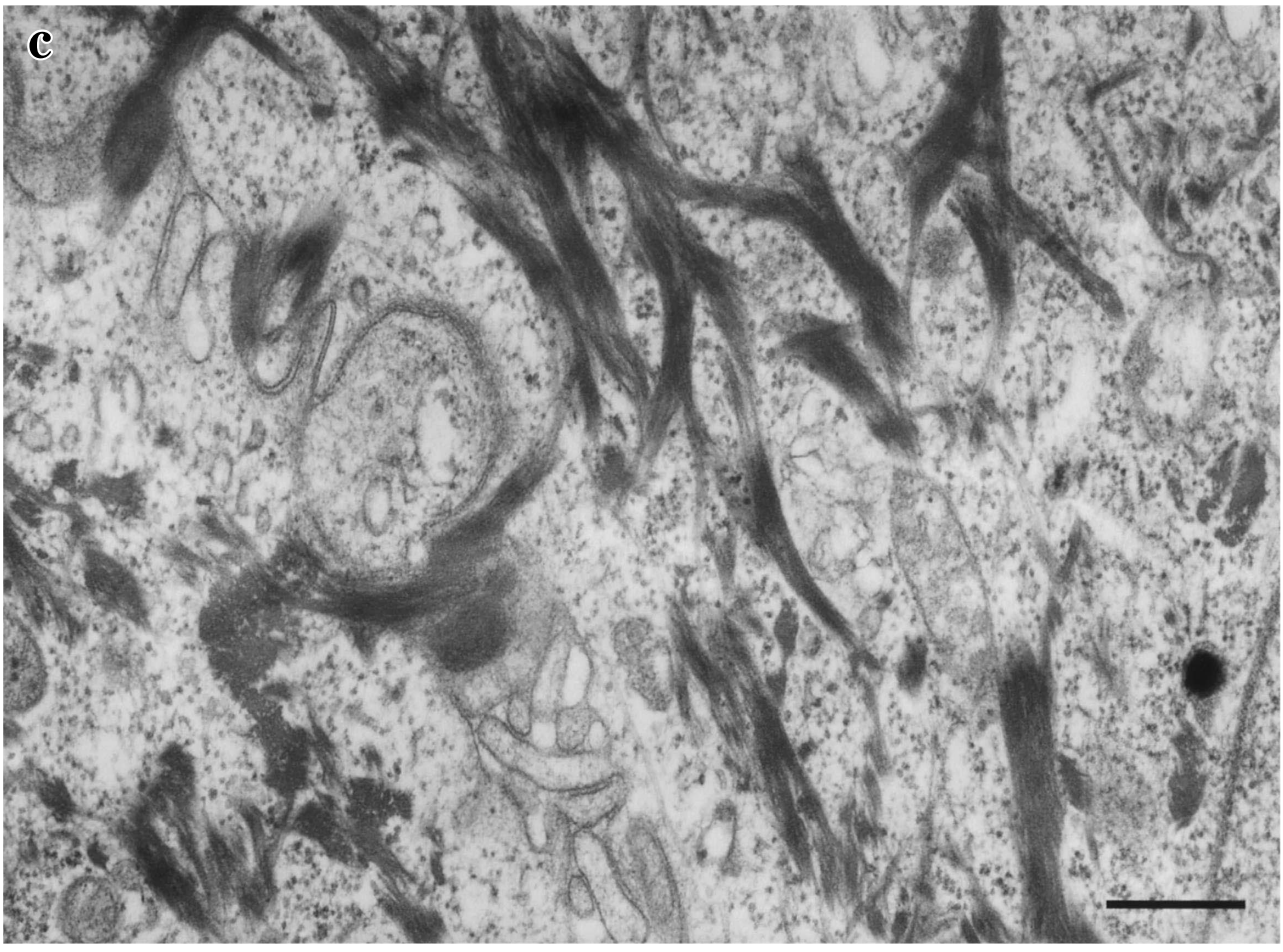

Fig. 6a, b, c. Group B processes had an extremely low electron density and few identifiable organelles, such as microtubules, some filaments, and mitochondria (bar=500 nm).
Fig. 6-a shows group B processes surrounded with the plasma membrane of a keratinocyte. Desmosomes can be seen with group B processes in Fig. 6-b. In Fig. 6-c, interdigitations of microvilli were found, and group B processes were adjacent to 2 plasma membranes of keratinocytes. They had few or no clefts in the spaces between adjacent keratinocytes.

leg. When we see axons without Schwann cells or a basement membrane in the epidermis, their physiological findings are quite doubtful. However, EM study showed that the positioning of IENFs toward keratinocytes in the intercellular space was similar to that of axons toward Schwann cells in other organs; keratinocytes probably play an alternate role of Schwann cells.

We conclude that EM can demonstrate the fine ultrastructural features of human IENFs and of surrounding structures in the intercellular space with little shrinkage of keratinocytes when 0.08 M of PB is used. Furthermore, differences in the cleft in the intercellular space of keratinocytes can be used to distinguish axons from other processes without ultrastructural immunohistochemical study. Therefore, the fine ultrastructural details will allow IENFs to be characterized more precisely and help clarify the pathogenesis of skin diseases.

Acknowledgement: We thank Carl Zeiss, Inc. Ltd., for confocal images.

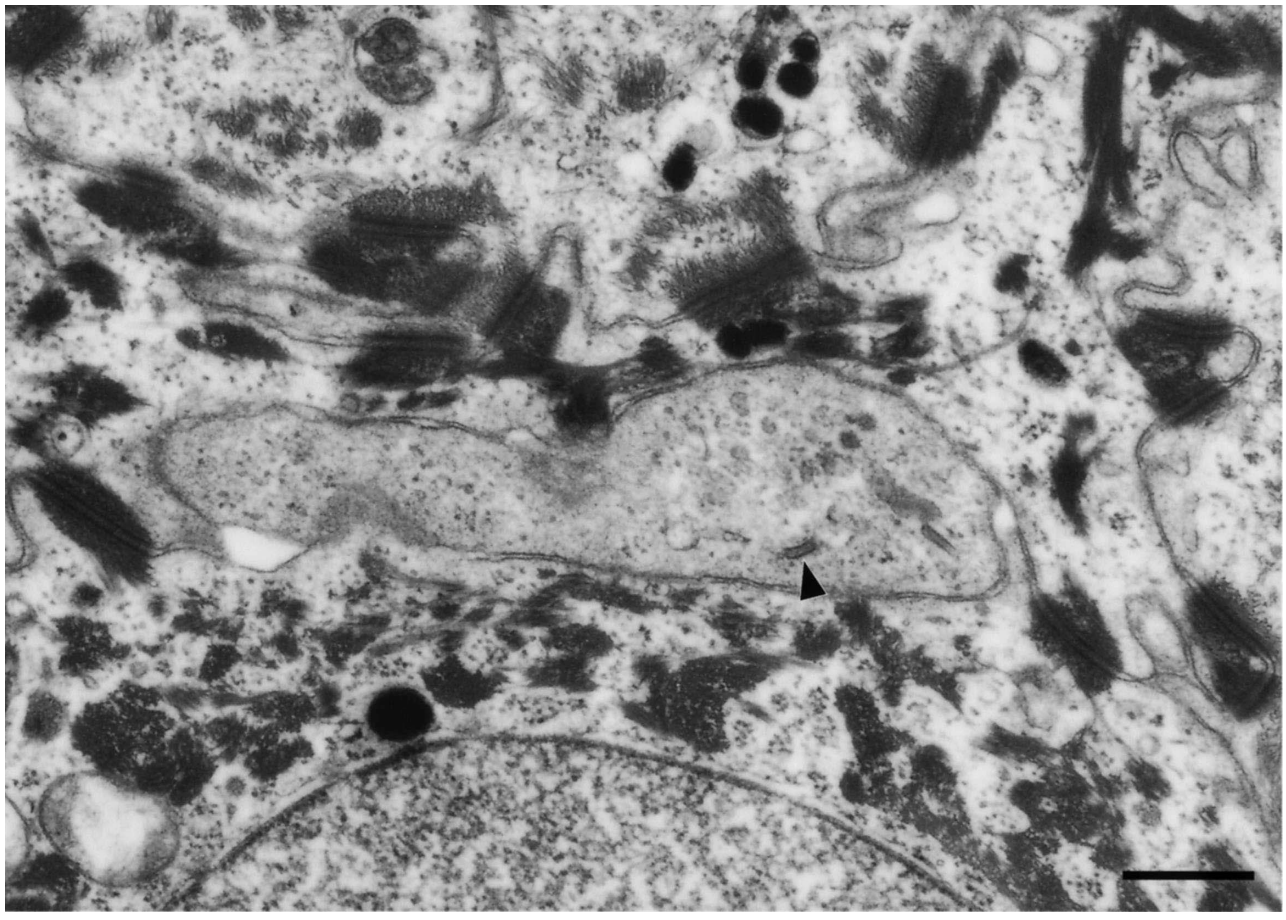

Fig. 7. Group C processes had a slightly low electron density with Birbeck granules (bar＝500 nm), did not have pinocytotic vesicles, and were adjacent to 4 membranes of keratinocytes with a nucleus of keratinocyte in below. They had some clefts in the intercellular spaces.

References

1. Langerhans P. Über die Nerven der menschlichen Haut. Virchows Arch 1868 ; 44 : 325–37.
2. Winkelmann RK. Some sensory nerve endings in skin : preliminary report on morphology of cutaneous sensation. AMA Arch Dermatol 1955 ; 71 : 373–8.
3. Arthur RP, Shelley WB. The innervation of human epidermis. J Invest Dermatol 1959 ; 32 : 397–410.
4. Cauna N. The effect of aging on the receptor organs of the human dermis. In Montagma W, editor : Advances in biology of skin. Vol. 6 New York : Pergamon Press ; 1964. p. 63–96.
5. Cauna N. Fine morphological characteristics and microtopography of the free nerve endings of the human digital skin. Anat Rec 1980 ; 198 : 643–56.
6. Novotony GEK, Gommert–Novotny E. Intraepidermal nerves in human digital skin. Cell Tissue Res 1988 ; 254 : 111–7.
7. Kennedy WR, Wendelschafer–Crabb G. The innervation of human epidermis. J Neurol Sci 1993 ; 115 : 184–90.
8. Kennedy WR, Wendelschafer–Crabb G, Johnson T. Quantitation of epidermal nerves in diabetic neuropathy. Neurology 1996 ; 47 : 1042–8.
9. Holland NR, Stocks A, Hauer P, Cornblath DR, Griffin JW, McArthur JC. Intraepidermal nerve fiber density in patients with painful sensory neuropathy. Neurology 1997 ; 48 : 708–11.
10. Lauria G, Holland N, Hauer P, Cornblath DR, Griffin JW, McArthur JC. Epidermal innervation : changes with aging, topographic location, and in sensory neuropathy. J Neurol Sci 1999 ; 164 : 172–8.
11. Nolano M, Provitera V, Crisci C, Stancanelli A, Wendelschafer–Crabb G, Kennedy WR, et al. Quantification of myelinated endings and mechanoreceptors in human digital skin. Ann Neurol 2003 ; 54 : 197–205.
12. Hirai T, Kanbe M, Honda H, Inoue K. Intraepidermal nerve fiber density and morphological characterization in 4 painful neuropathy patients. Peripheral Nerve 2006 ; 17 : 239–41.

Fig. 8. Group D processes had many organelles with pinocytotic vesicles and melanosomes. They were adjacent to 3 membranes of keratinocytes with 3 nuclei. They had some clefts in the intercellular spaces (bar=500 nm).

13. Hilliges M, Wang L, Johansson O. Ultrastructural evidence for nerve fibers within all vital layers of the human epidermis. J Invest Dermatol 1995; 104: 134–7.
14. Luft JH. Improvements in epoxy resin embedding methods. J Biophys Biochem Cytol 1961; 9: 409–14.
15. Wendelschafer-Crabb G, Walk D, Foster S, Kennedy WR. Epidermal nerve fiber densities in six body locations of normal and diabetic subjects. J Periph Nerv Sys 2005; 10 (supplement): 104.